THE BELL SYSTEM TECHNICAL JOURNAL
Vol. 53, No. 7, September 1974
Printed in U.S.A.

An Improved Antenna for Microwave Radio Systems Consisting of Two Cylindrical Reflectors and a Corrugated Horn

By C. DRAGONE

(Manuscript received January 31, 1974)

A broadband antenna is described with an elliptical beam suitable for efficient illumination of the United States from a satellite in synchronous orbit. The antenna is also suitable for use in terrestrial radio systems above 10 GHz. It consists of a corrugated feed and two parabolic cylinders that efficiently transform the circularly symmetric beam radiated by the feed into an elliptical beam. Depolarization of the incident beam by the two cylinders is very small and essentially independent of the angle of incidence, which can therefore be chosen as large as required to avoid aperture blockage.

The performance is described of an antenna with a 5.8° × 2.9° elliptical beam at 18.5 GHz. For any input polarization, the cross-polarized component of the far field remains over the entire beam at least 33.5 dB below the main component on axis. This cross-polarized component is due in part to imperfections in the corrugated feed and in part to some aperture blockage by the feed and depolarization by the cylinders.

A first-order analysis of the frequency dependence shows that the beamwidths vary little with frequency for an antenna using a properly designed feed and cylinders of sufficiently large apertures. As the frequency is increased from 18.5 to 29 GHz, the measured horizontal and vertical beamwidth variations are +2.7 and −1.4 percent, respectively.

I. INTRODUCTION

The suitability of corrugated feeds for use in reflector antennas of revolution is well known.[1,2] When this feed is properly designed, the resulting far field of the antenna is a circularly symmetric beam reproducing, in all directions, the input polarization of the feed. It is shown here that this feed is also suitable for use with orthogonal

cylinders, with excellent performance. Although the far field in this case has a cross-polarized component resulting from depolarization by the cylinders, this component is very small, negligible for most applications. An important advantage of cylindrical reflectors over reflectors of revolution* is that this cross-polarized component is essentially independent of the angle of incidence, for incidence in a plane orthogonal to the axis of the first cylinder. Because of this property, aperture blockage can be eliminated by properly orienting the feed without sacrificing the polarization properties of the antenna.

We describe the performance of an antenna consisting of two orthogonal parabolic cylinders[4] and a corrugated feed (Fig. 1). The two cylinders transform the circularly symmetric beam radiated by the feed into an elliptical beam. Thus, this antenna is particularly suitable for applications requiring different beamwidths in the two principal planes. One such application arises when a satellite in synchronous orbit is required to efficiently illuminate a region of approximately elliptical shape, such as the United States. Another application[5] arises in connection with terrestrial microwave radio systems above 10 GHz, where an important limitation arises in the use of antennas with very narrow beams, because of the finite stability of the towers on which the antennas are to be mounted. In that case, the choice of beamwidth in a vertical plane may be governed by the maximum movement of the tower in heavy wind, and it may therefore be desirable[5] to choose different values for the beamwidths in the two principal planes.

In Fig. 1a the two parabolic cylinders are so arranged† that, if a point source is placed at F in front of the first cylinder, a spherical wave is transformed by the two cylinders into a plane wave. This implies that the focal point F lies on the focal line of the first cylinder. The spherical wave is therefore transformed by this reflector into a cylindrical wave originating from a virtual line source behind the reflector (see Fig. 1a). The second reflector, which is disposed so that its focal line coincides with the line source, then transforms the cylindrical wave into a plane wave. All this means that the rays from F that are intercepted by the first cylinder become, after the two reflections, parallel rays, i.e., rays focused at infinity. Because of this property, it can be shown that if the two cylinders are of sufficiently

* The polarization properties of reflectors of revolution for oblique incidence are discussed in Ref. 3.

† Details of the geometry of the two cylinders and their transformations are given in Ref. 4.

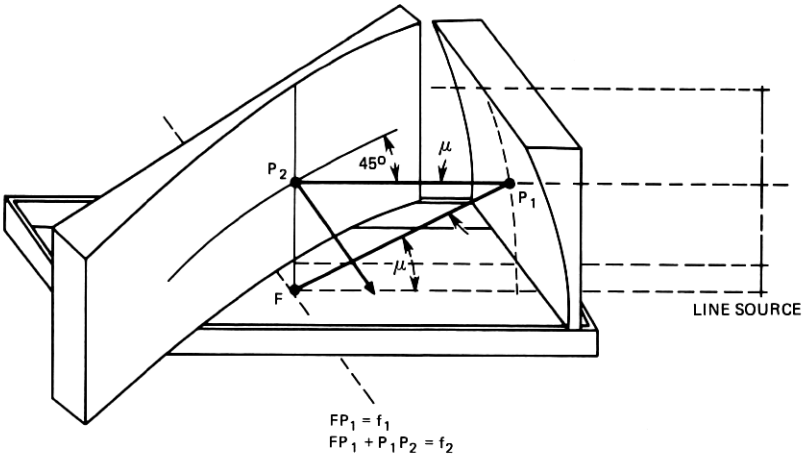

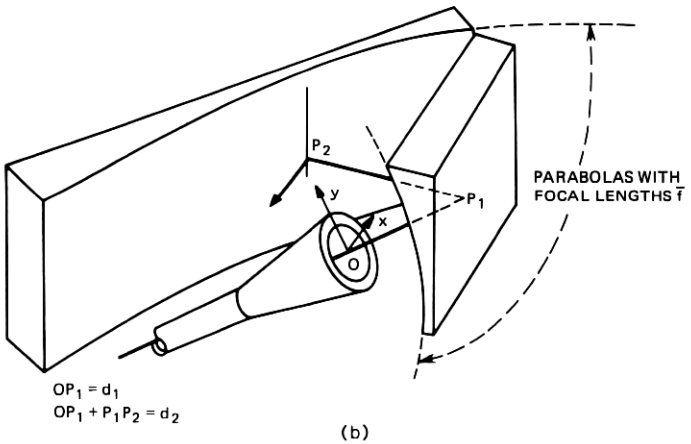

Fig. 1—Double cylinder antenna (a) with feed removed and (b) with feed shown. $FP_1 = f_1$, $FP_1 + P_1P_2 = f_2$, $FQ_1 = f$; $OP_1 = d_1$, $OP_1 + P_1P_2 = d_2$.

large aperture there is a simple relation[6] between the far field and the field over the focal plane Σ_0, which is the plane orthogonal to the feed axis at F. More precisely, consider a plane Σ_1 orthogonal to the beam at a great distance from the antenna. To a first order, Σ_0 and Σ_1 are conjugate planes and therefore their field intensities can be determined

accurately using the imaging laws of geometrical optics.* Since the magnifications of Σ_1 in the horizontal and vertical directions are proportional to the focal lengths f_1 and f_2, respectively, it follows that the circularly symmetric field radiated on Σ_0 by the feed is imaged into an elliptical beam whose beamwidths in the two principal planes have the ratio

$$r = \frac{f_1}{f_2}. \tag{1}$$

An important consequence of the relation of far field to focal plane field is that, since the field distribution over the aperture of a properly designed feed varies little with frequency and since the feed aperture is normally placed close to the focal plane, the beam of the antenna is essentially frequency independent. This can be an important property in many applications. We now derive the antenna characteristics under the assumption that the wave transformation by the two cylinders is efficient, i.e., that each cylinder intercepts essentially all the energy incident on it.

II. ANALYSIS

Throughout this section we assume that the feed radiates a narrow beam. This implies that the radius a of the circular feed aperture is much larger than the wavelength λ,

$$ka \gg 1,$$

where $k = 2\pi/\lambda$.

Suppose the wave incident on the first cylinder is a spherical wave originating from the focal point F. According to geometrical optics, this wave is transformed by the two cylinders into a plane wave having the following characteristics.[4] If, for the incident wave,

$$E_x = 0, \tag{2}$$

then the resulting plane wave is vertically polarized; if, instead,

$$H_x = 0, \tag{3}$$

then the plane wave is horizontally polarized. In the first part of this section, we assume the former condition.

Since the feed radiates a narrow beam, consideration can be restricted to the field in the paraxial region of the principal ray, which

* This result is derived in Ref. 6 for systems having rotational symmetry and is extended in Appendix A to the asymmetric system of Fig. 2.

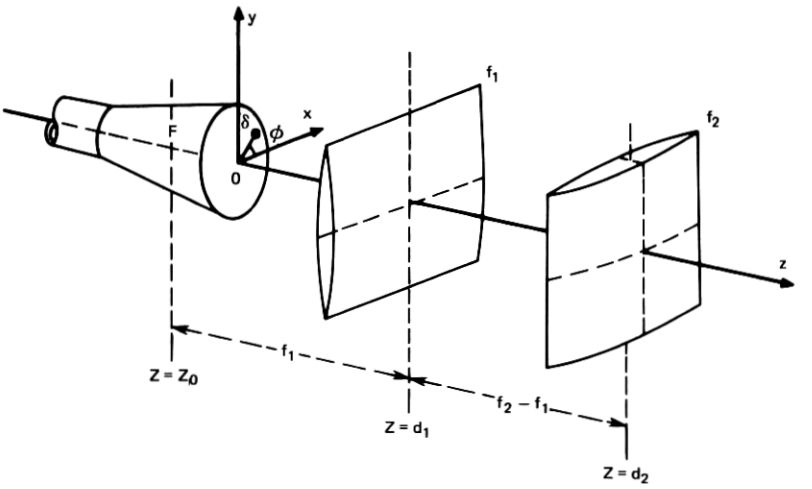

Fig. 2—System consisting of a feed and two ideal cylindrical lenses.

is the ray that corresponds to the feed axis. The system of Fig. 1b can then be replaced by the fictitious system of Fig. 2, consisting of two cylindrical lenses of focal lengths, f_1, f_2. The lenses in Fig. 2 are assumed ideal; they simply multiply the incident field by the phase factors

$$\exp\left(-j\frac{k}{2f_1}x^2\right) \quad \text{and} \quad \exp\left(-j\frac{k}{2f_2}y^2\right). \tag{4}$$

The distances, d_1, d_2, of the two lenses from the feed aperture are the distance in Fig. 1b between the two reflectors and the feed aperture, measured along the principal ray. We assume that the separation $d_2 - d_1$ between the two lenses is equal to $f_2 - f_1$,

$$d_2 - d_1 = f_2 - f_1, \tag{5}$$

so that the focal lines of the two lenses coincide. Then a spherical wave originating from the point $z = z_0$, where

$$z_0 = d_1 - f_1 = d_2 - f_2, \tag{6}$$

is transformed by the two lenses into a plane wave. The rectangular system of x, y, z coordinates in Fig. 2 has been chosen so that the feed aperture lies in the $z = 0$ plane centered at $x = y = z = 0$.

The following correspondence exists between the two systems of Figs. 1b and 2. Let s be a parameter measuring distance from the center of the feed aperture along the principal ray of Fig. 1b. Then

the field distribution over a plane normal to the principal ray at some point $s = s'$ is given by the field in Fig. 2 over the corresponding plane $z = s'$. This correspondence is, of course, valid only in the neighborhood of the principal ray.

2.1 Field for $z \to \infty$

Using the Fresnel diffraction formula,* a simple expression for the far field is derived in Appendix A, relating the far field to the focal plane field. Consider a plane $z = z_1$ at a great distance from the antenna. Because of condition (5), the planes $z = z_0$ and $z = z_1$ are conjugate planes. If x_0, y_0, z_0 and x_1, y_1, z_1 are corresponding points over these two planes, it follows from eq. (32) of Appendix A that

$$|E_y(x_1, y_1, z_1)| \to \frac{\sqrt{f_1 f_2}}{z_1} \left| E_y\left(\frac{x_1}{M_x}, \frac{y_1}{M_y}, z_0\right)\right|, \tag{7}$$

where M_x and M_y are the magnifications in the xy-directions,

$$M_x = \frac{x_1}{x_0} = -\frac{z_1}{f_1}, \qquad M_y = \frac{y_1}{y_0} = -\frac{z_1}{f_2}. \tag{8}$$

Thus, the far field is given by the field over the focal plane $z = z_0$. Since in practice this plane is not too far from the aperture plane of the feed, its field distribution can be determined accurately with little difficulty, using the Fresnel diffraction formula or the procedure of Appendix B.

2.2 Feed characteristics

The corrugated feed is a conical horn with circular symmetry. Its aperture is illuminated by the fundamental mode of the horn, which is a spherical hybrid mode[9] generated from a TE_{11}-mode of a smooth waveguide by a transducer† connected to the input of the horn. Let (ρ, ϕ) be polar coordinates defined by $x = \rho \cos \phi$, $y = \rho \sin \phi$ (see Fig. 2) and assume the input TE_{11}-mode is vertically polarized. Then we can show that the vertical component of the field over the aperture

---

* Fresnel's formula is applicable provided the wave equation $(k^2 + \partial^2/\partial x^2 + \partial^2/\partial y^2 + \partial^2/\partial z^2)E_y = 0$ can be approximated by the parabolic wave equation (Ref. 7)

$$[k^2 + \tfrac{1}{2}(\partial^2/\partial x^2 + \partial^2/\partial y^2)]E_y = -jk\partial E_y/\partial z.$$

This approximation is justified in our case (we assume $ka \gg 1$; $f_1, f_2 \gg a$), since the field radiated by the feed is made up of plane waves whose directions of propagation are mostly confined to a small angular region about the z-axis (Ref. 8).

† Details of the feed and the transducer, which are of standard design, are not given here.

is given accurately by the function

$$\psi = \psi(\rho) = J_0(u) \exp\left(jk \frac{\rho^2}{2R}\right), \tag{9}$$

where J_0 is the Bessel function of order zero and

$$u = \frac{\rho}{a} u_{\alpha 0},$$

$u_{\alpha 0}$ being the first zero of $J_0(u)$,

$$J_0(u_{\alpha 0}) = 0, \qquad u_{\alpha 0} = 2.4048.$$

The factor $\exp[jk(\rho^2/2R)]$ in eq. (9) arises because the hybrid mode illuminating the feed aperture has a spherical phase front with radius of curvature R approximately equal to the length of the horn from vertex to aperture. Equation (9) is true provided $R \gg a$, a condition approximately satisfied in the experiment ($R \cong 4.17\ a$). Note that $\psi = 0$ for $\rho = a$. This is due to the corrugated wall that imposes to a good approximation the boundary condition

$$E_\phi = H_\phi = 0, \tag{10}$$

where E_ϕ, H_ϕ are the components of E, H in the ϕ-direction. Appendix C shows that a consequence of this condition is that the field over the aperture contains, in addition to the component $E_y = \psi(\rho)$, a small component given accurately by

$$E_x \cong \frac{1}{2k^2} \cdot \frac{\partial^2 E_y}{\partial x \partial y}. \tag{11}$$

As a consequence, the far field contains a small (undesirable) horizontal component* that can be determined accurately by replacing the system of Fig. 1 by that of Fig. 2. The amplitude of this component is therefore given by a formula analogous to eq. (7) [simply replace E_y with E_x in eq. (7)].

2.3 First-order polarization properties of the far field

The location of the feed is normally chosen so that its phase center, the center of curvature P_c of the phase fronts of the far field, coincides with the focal point $z = z_0$ of the two reflectors. We assume this condition. Consider first the ideal case $R = \infty$, in which P_c is at the center

* Actually, E_x also causes a small vertical component. This component is, however, much smaller (for large ka) than the vertical component resulting from E_y and can therefore be neglected.

of the feed aperture and therefore the aperture is placed in the focal plane. Then, over this plane, E_y is given by $\psi(\rho)$ and eq. (7) gives for the far field

$$|E_y| \to \frac{\sqrt{f_1 f_2}}{z} |\psi(v)|, \tag{12}$$

where

$$v = \sqrt{\xi^2 + \eta^2}, \qquad \xi = \frac{x f_1}{z}, \qquad \eta = \frac{y f_2}{z}. \tag{13}$$

A relation identical to eq. (7) can be written for E_x. Therefore, since, for $z = 0$, E_x is given by eq. (11),

$$|E_x| \to \frac{\sqrt{f_1 f_2}}{z} \frac{1}{2k^2} \left| \frac{\partial^2 \psi}{\partial \xi \partial \eta} \right| = \frac{\sqrt{f_1 f_2}}{2} \frac{1}{2k^2} \left| \frac{\xi \eta}{v^2} \left(\psi''(v) - \frac{\psi'(v)}{v} \right) \right|. \tag{14}$$

We note from this relation that $|E_x|$ attains its maximum value for $\xi = \eta = v_0/\sqrt{2}$, where v_0 is the value of v for which $|\psi''(v) - \psi'(v)/v|$ is maximum. In the particular case of eq. (9), with $1/R = 0$,

$$|\psi| = \left| J_0 \left(\frac{u_{a0}}{a} v \right) \right|, \tag{15}$$

$$|\psi''(v) - \psi'(v)/v| = \left(\frac{u_{a0}}{a} \right)^2 \left| J_2 \left(\frac{u_{a0}}{a} v \right) \right|, \tag{16}$$

for $v < a$. We can verify that the maximum value of J_2 in the interval $v \leqq a$ occurs for $v = a$ and is $J_2(u_{a0}) = 0.431$. Therefore, if C denotes the ratio between the peak of $|E_x|$ and the peak of $|E_y|$ (the peak of $|E_y|$ occurs on axis), using eqs. (12), (14), (15), and (16), we find

$$C = \frac{|E_x|_{\max}}{|E_y|_{\max}} = \frac{1}{4} \left(\frac{u_{a0}}{ka} \right)^2 J_2(u_{a0}) \cong \frac{0.6231}{(ka)^2}. \tag{17}$$

Next, consider the case $1/R \neq 0$ but, instead of considering the distribution of eq. (9), assume that E_y over the aperture plane $z = 0$ varies as

$$\exp\left(-\frac{\rho^2}{w^2} \right) \exp\left(jk \frac{\rho^2}{2R} \right). \tag{18}$$

Appendix B points out that, for

$$w \cong 0.6437a, \tag{19}$$

this distribution represents fairly accurately that of eq. (9).

The phase center P_c (and, therefore, the focal plane) is now behind the aperture of the feed, located at[6,10]

$$z_0 = -\frac{R}{1 + (\lambda R/\pi w^2)}, \tag{20}$$

and we can verify that, over the plane $z = z_0$, E_y varies as

$$\psi_0 = \exp\left(-\frac{\rho^2}{w_0^2}\right),$$

where[6,10]

$$w_0^2 = \frac{w^2}{1 + (w^2\pi/\lambda R)^2}. \tag{21}$$

Since the maximum value of $|\psi_0'' - \psi_0'/\rho|$ occurs for $\rho = w_0$ and is

$$|\psi_0'' - \psi_0'/\rho|_{\max} = \frac{4}{ew_0^2}, \tag{22}$$

the ratio C between $|E_x|_{\max}$ and $|E_y|_{\max}$ is now given by

$$C = \frac{1}{e(kw_0)^2}. \tag{23}$$

To allow a direct comparison of eqs. (23) and (17), let us assume $1/R = 0$ and w given by eq. (19). From eqs. (19) and (23) we get

$$C = \frac{0.889}{(ka)^2}, \tag{24}$$

which gives values somewhat larger than eq. (17).

In the case of the experiment $a \cong 2.35\ \lambda$, $R = 9.78\ \lambda$. For these values of a, R, from eqs. (19), (21), and (23), we obtain, for C^2, -44 dB. This, of course, is only a rather crude estimate of the actual depolarization by the two cylinders (the mean square error in representing the actual distribution (9) by means of (18) is almost 2 percent; see Appendix B). For the present purpose, however, this estimate is quite adequate, since in the experiment other effects such as imperfections in the feed and some aperture blockage by the feed are found to be predominant.

III. EXPERIMENT

Two mirrors and a feed were constructed and assembled as shown in Fig. 3. Their radiation characteristics were measured at 18.5 GHz. The cylindrical surfaces of the two mirrors were milled to a tolerance

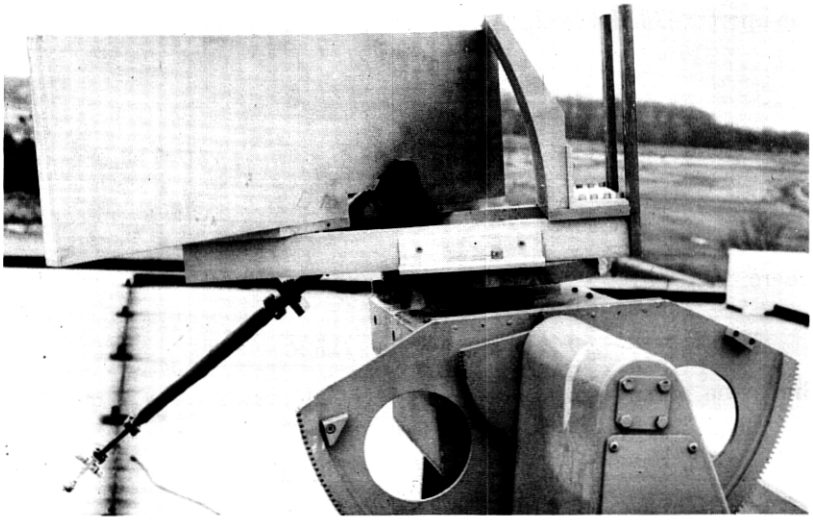

Fig. 3—Double cylinder antenna with corrugated feed.

of about 1 mil. The parabolas generating the two cylinders have the same focal length $\bar{f} = 12.919\ \lambda$.

The feed, a corrugated horn with

$$ka = 14.76, \qquad R = 4.17\ a, \tag{25}$$

satisfies the boundary condition (10) at 18.5 GHz, and therefore its radiation pattern is essentially circularly symmetric.[1,2] A measured pattern is shown in Fig. 4. Figure 4 also shows the pattern calculated for the gaussian distribution (18), with w given by eq. (19). The two patterns are somewhat different, as expected, since the distribution (18) represents only the fundamental term ($m = 0$) of eq. (35). A much closer agreement with the measured pattern could be obtained from eq. (35) by considering also the term relative to $m = 2$ (it turns out that the term $m = 1$ is negligible), but for the present purpose the accuracy of Fig. 4 is satisfactory.

If we consider only the fundamental term (18), the location of the phase center P_c and the beamwidth of the feed can be calculated straightforwardly by using eqs. (20) and (47); the 3-dB beamwidths of the antenna in the principal planes are given by eqs. (45) and (46) of Appendix B.

The distance z_0 of the feed aperture from the focal point F was chosen using eq. (20), in which case the phase center P_c of (18) coin-

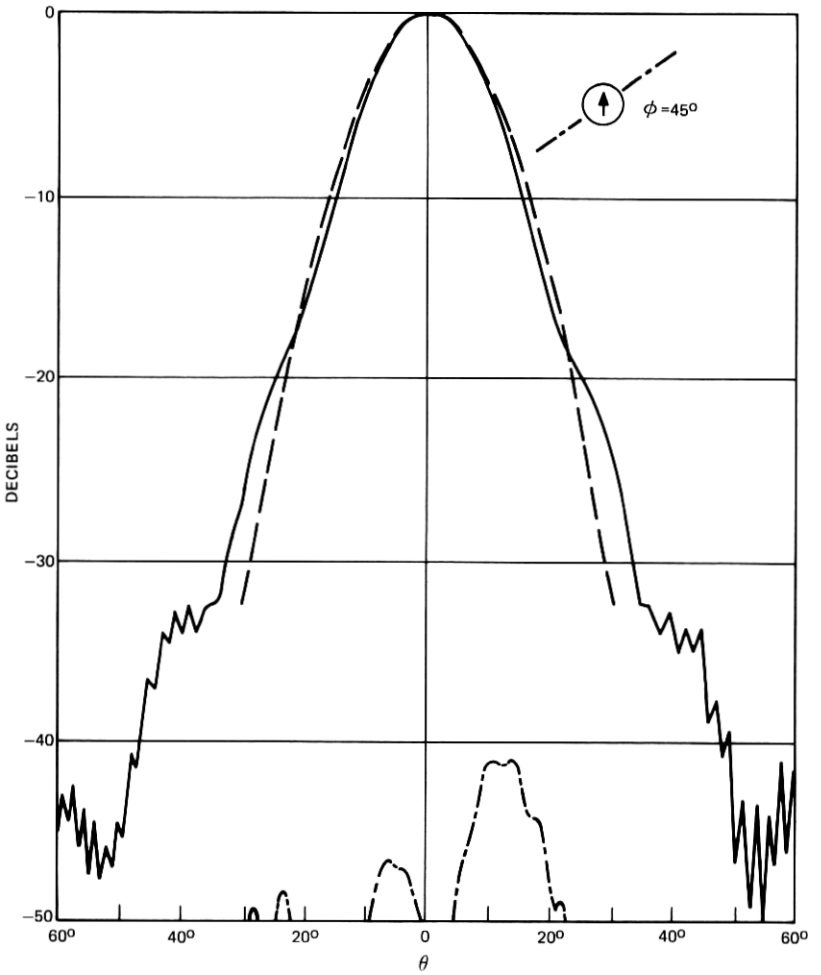

Fig. 4—Radiation patterns of vertically polarized corrugated feed measured at 18.5 GHz in the $\phi = 45°$ plane for the main component (——) and the cross-polarized component (–·–·–) of the far field. The curve (– – – –) is the pattern calculated for the gaussian distribution of eqs. (31) and (32).

cides with F. We can show, using eqs. (46) and (47), that under this condition the beamwidths of the antenna are stationary with respect to small displacements of the feed. The orientation of the feed with respect to the first cylinder was chosen as follows.

When the angle of incidence μ in Fig. 1 is 0, which is the condition assumed in Ref. 4, the axis of the beam reflected by the first cylinder

coincides with the axis of the feed. Because of the relatively large size of the feed aperture, this condition ($\mu = 0$) is undesirable, since a relatively large fraction of the energy reflected by the first cylinder is then intercepted by the feed aperture. Thus, in the experiment, a relatively large value (36°) was chosen for μ. For this value, the energy blocked by the feed is small. Using the distribution of eq. (18), we

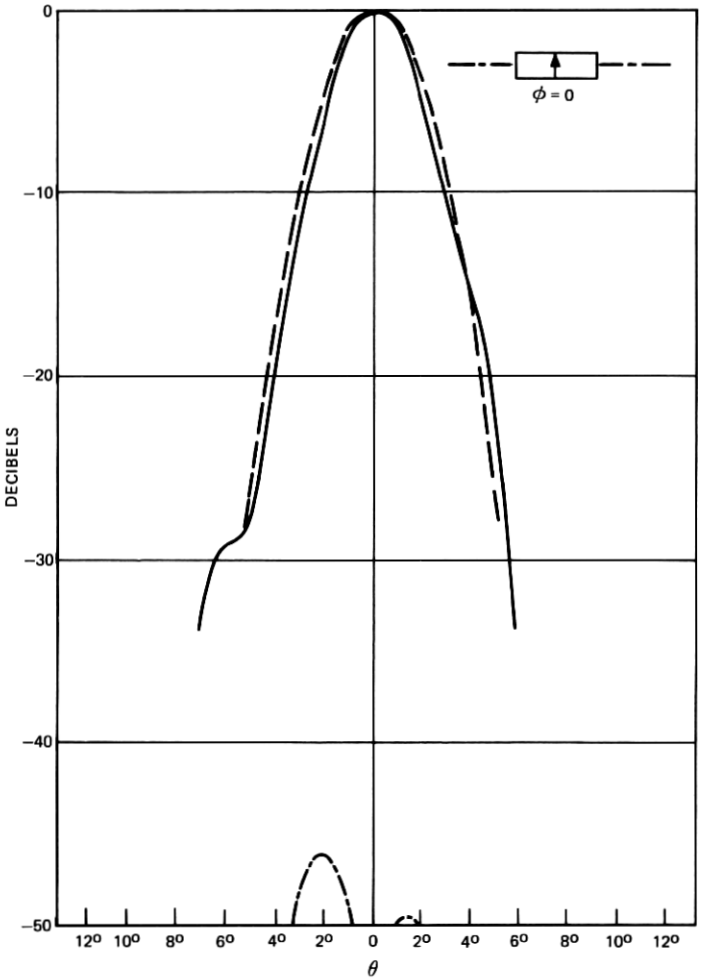

Fig. 5—Radiation patterns of vertically polarized double-cylinder antenna measured at 18.5 GHz in the horizontal plane $\phi = 0$ for the main component (——) and the cross-polarized component (–·–·–) of the far field. Curve (– – – –) is the pattern calculated from eq. (18) for the gaussian distribution of eqs. (31) and (32).

can show that the field incident on the upper edge of the feed is about -10 dB with respect to the field on the axis of the incident beam.

The first cylinder in Fig. 3 (14.91 λ by 14.32 λ) intercepts most radiation from the feed; the illumination of its four edges with respect to the illumination at the center is less than -16.5 dB on the upper edge and less than -24.5 dB on the other three edges.

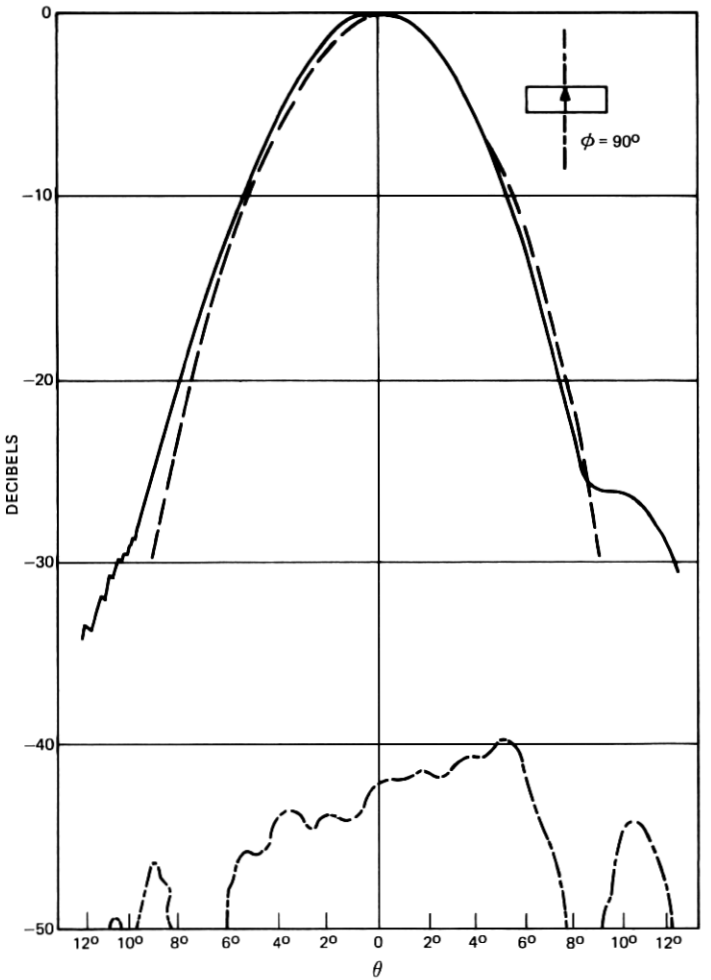

Fig. 6—Radiation patterns of vertically polarized double-cylinder antenna measured at 18.5 GHz in the vertical plane $\phi = 90°$ for the main component (——) and the cross-polarized component (–·–·–) of the far field. Curve (– – – –) is the pattern calculated from eq. (18) for the gaussian distribution of eqs. (31) and (32).

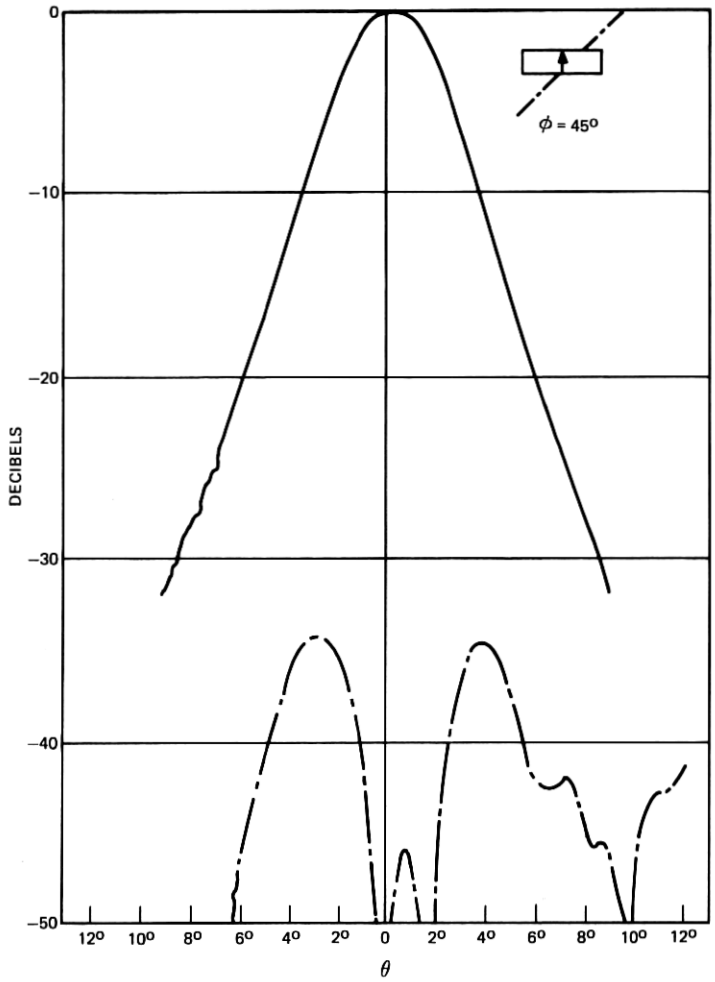

Fig. 7—Radiation patterns of vertically polarized double-cylinder antenna measured at 18.5 GHz in the $\phi = 45°$ plane for the main component (——) and the cross-polarized component (–·–·–) of the far field.

The second reflector (44.77 λ by 14.32 λ) is sufficiently large that it intercepts essentially all the energy reflected by the first cylinder, except for the energy blocked by the feed. The distances f_1, f_2 measured along the principal ray between F and the two reflectors are* 14.282 λ

* We can show (see Ref. 4) that

$$f_1 = \frac{2\hat{f}}{1 + \cos\mu}$$
$$f_2 = 2\hat{f}.$$

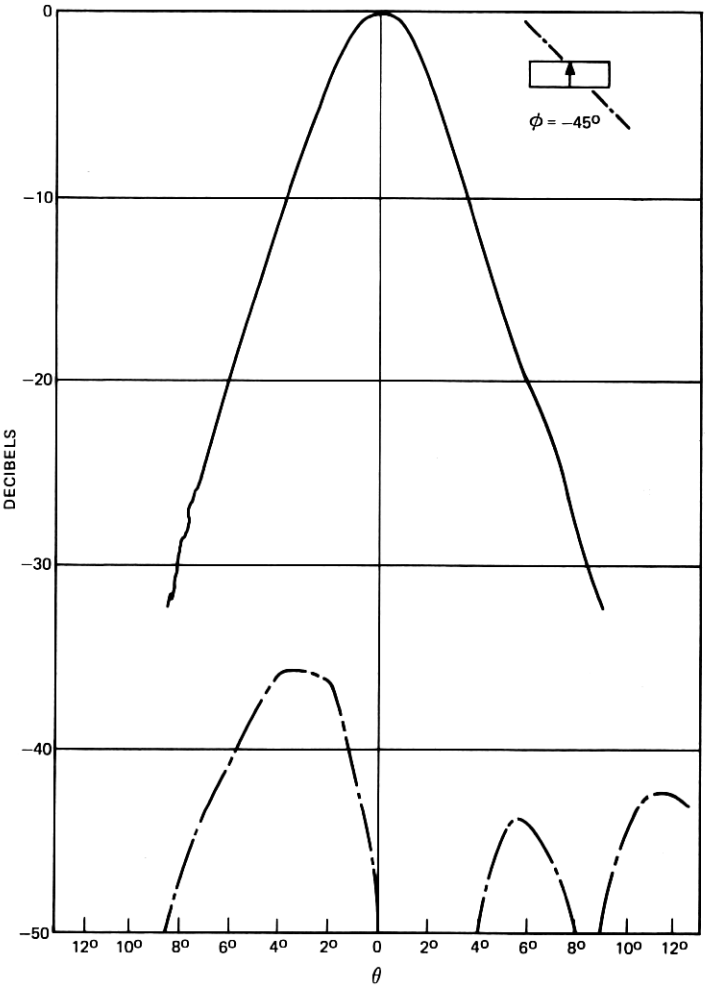

Fig. 8—Radiation patterns of vertically polarized double-cylinder antenna measured at 18.5 GHz in the $\phi = -45°$ plane for the main component (——) and the cross-polarized component (-·-·-) of the far field.

and 25.837 λ. Since $d_1 = f_1 + z_0$ and $d_2 = f_2 + z_0$, using eqs. (46) and (47), we obtain for the beamwidths in the two principal planes

$$2\theta_1 = 5.75°, \qquad 2\theta_2 = 3.18°.$$

The measured values (Figs. 5 and 6) are $2\theta_1 = 5.84°$ and $2\theta_2 = 2.87°$.

Figures 5 to 8 show the measured patterns in the principal planes $\phi = 0$, $\phi = 90°$ and in the planes $\phi = 45°$, $\phi = -45°$. In these figures, θ is the angle from the beam axis. Also shown in Figs. 5 and 6

are patterns calculated for the distribution (18). In all these cases, the feed is vertically polarized; the main patterns of Figs. 5 to 8 (the solid curves) give, therefore, the magnitude of the vertical component E_y, in dB with respect to the field on axis.

The patterns for the horizontal component E_x are given in Figs. 5 to 8 by the dashed curves. In the worst case, the plane $\phi = 45°$, the

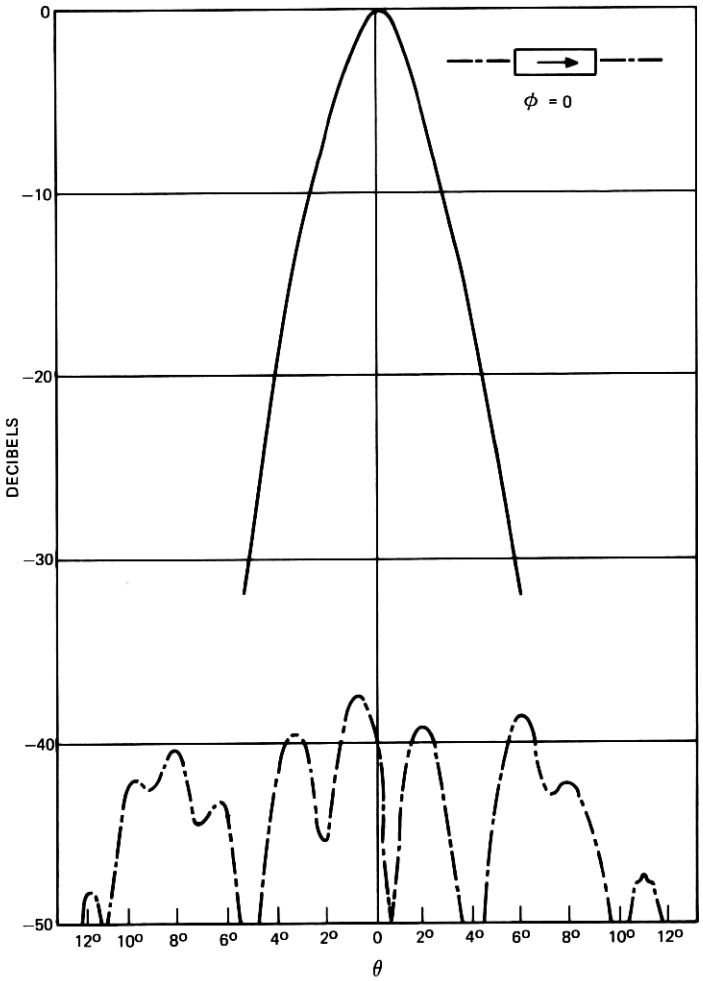

Fig. 9—Radiation patterns of horizontally polarized double-cylinder antenna measured at 18.5 GHz in the horizontal plane $\phi = 0$ for the main component (——) and the cross-polarized component (–·–·–) of the far field.

ratio C between the largest value of $|E_x|$ and the peak of $|E_y|$ is -33.5 dB, which is approximately 10.5 dB larger than the value given by eq. (23). This larger value of C is due in part to blockage by the feed and in part to imperfections in the feed that were found to cause a cross-polarized component in the feed radiation patterns with a peak of approximately -41 dB (see Fig. 4). The effect of blockage by the

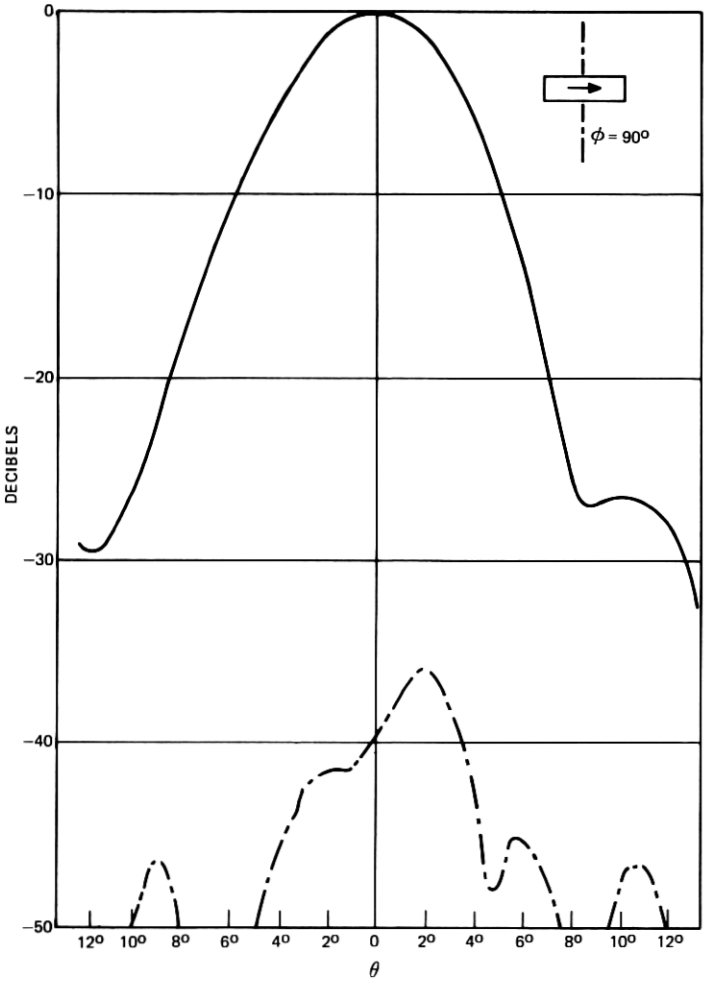

Fig. 10—Radiation patterns of horizontally polarized double-cylinder antenna measured at 18.5 GHz in the vertical plane $\phi = 90°$ for the main component (——) and the cross-polarized component (-·-·-) of the far field.

feed was evaluated by measuring the variation of C with μ. Decreasing μ from 36° to 31° caused an increase in C of approximately 3 dB.

The radiation patterns for a horizontally polarized feed are shown in Figs. 9 to 12. The cross-polarized component now has a peak of −35 dB in the worst case, the $\phi = 45°$ plane, which is about 1.5 dB lower than the value measured for vertical polarization.

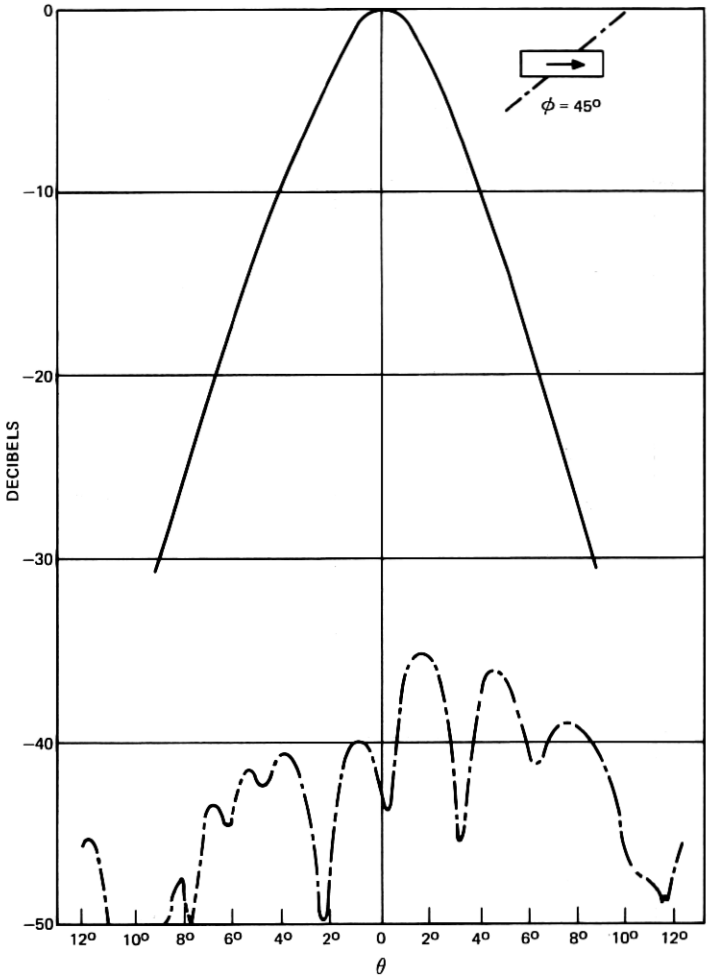

Fig. 11—Radiation patterns of horizontally polarized double-cylinder antenna measured at 18.5 GHz in the $\phi = 45°$ plane for the main component (——) and the cross-polarized component (–·–·–) of the far field.

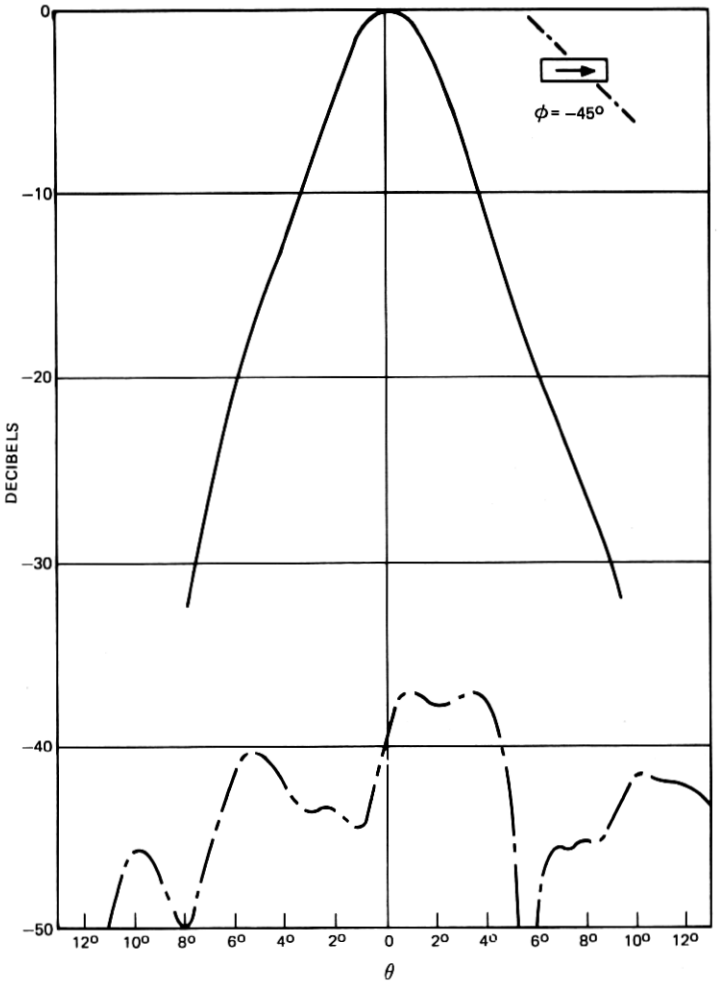

Fig. 12—Radiation patterns of horizontally polarized double-cylinder antenna measured at 18.5 GHz in the $\phi = -45°$ plane for the main component (——) and the cross-polarized component (–·–·–) of the far field.

In all the above measurements, the frequency was 18.5 GHz. Measurements at 29 GHz were also made to determine the frequency dependence of the two beamwidths $2\theta_1$, $2\theta_2$. At 29 GHz the measured values of $2\theta_1$ and $2\theta_2$ with the feed vertically polarized were $2\theta_1 = 6°$ and $2\theta_2 = 2.47°$. Thus, $2\theta_1$ increased by only 2.7 percent, with respect to the value measured at 18.5 GHz, while $2\theta_2$ decreased by 14 percent.

This difference in the variation of $2\theta_1$ and $2\theta_2$ is due to the lack of feed pattern symmetry as the frequency was increased. At 29 GHz in the H- and E-planes, $2\theta_{f1}$ was greater than $2\theta_{f2}$ by approximately 10 percent.

IV. CONCLUSIONS

Cylindrical reflectors are well adapted to efficiently generate an elliptical beam from the circularly symmetric beam radiated by a corrugated feed. Depolarization by the cylinders is negligible (10 $\log_{10} C^2 < -40$ dB, for $a > 1.25\ \lambda$) for typical feed diameters, and it is essentially independent of the angle of incidence μ which can therefore be chosen as large as needed to minimize aperture blockage.

In the experiment, blockage by the feed,* although small, was large enough to cause some deterioration in C^2. The measured value of C^2 in the worst case was -33.5 dB, approximately 10.5 dB higher than the value given by eq. (23). This higher value was due in part to certain imperfections in the feed.

A first-order analysis of the antenna was given in Section II. It was pointed out that, if the feed aperture is located close to the focal point F, then the beamwidths θ_1 and θ_2 vary little with frequency, assuming that each reflector intercepts all the energy incident on it. Simple approximate expressions [eqs. (45) and (46)] were given for θ_1 and θ_2. The measured values, $2\theta_1 = 5.8°$ and $2\theta_2 = 2.9°$ agree well with the values given by those equations.

V. ACKNOWLEDGMENTS

Thanks are due to Mrs. D. Vitello for programming the calculations of $\bar{u}$ and η_{max} of eqs. (38) and (39). The measurements were carried out by W. E. Legg.

APPENDIX A

This appendix derives the field transformation through the two lenses of Fig. 2. Consider first the one-dimensional case of Fig. 13, where it is assumed that E_y is a function of only x, z,

$$E_y = E_1(x, z)e^{jkz}.$$

Let the problem be to find E_y over the image plane $z = z_1$, with E_y

* The antenna considered here has an unusually large ($\approx$2.75) ratio of focal distance to feed diameter (this is mainly due to the relatively large value required of θ_1). If a much narrower beam is desired, aperture blockage can be entirely eliminated without difficulty.

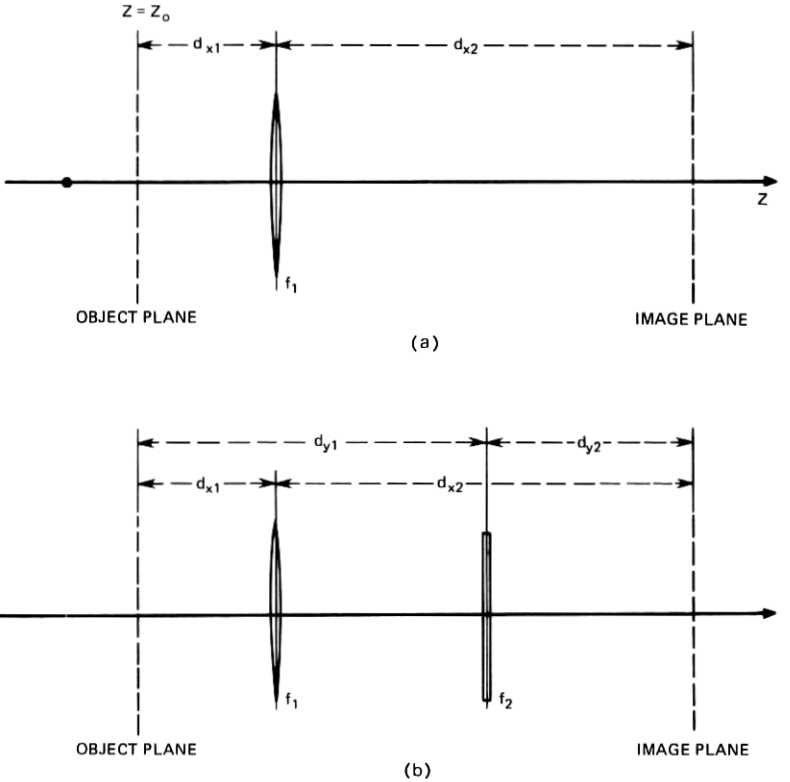

Fig. 13—Imaging (a) of one-dimensional field distribution by a cylindrical lens and (b) of two-dimensional field distribution by two orthogonal cylindrical lenses.

given [by some function $\psi_1(x)$] over the object plane $z = z_0$,

$$E_1(x, z) = \psi_1(x) \qquad \text{for} \quad z = z_0.$$

The distances d_{x1} and d_{x2} between the cylindrical lens and object and image planes are related by

$$\frac{1}{d_{x1}} + \frac{1}{d_{x2}} = \frac{1}{f_1}, \tag{26}$$

where f_1 is the focal length of the lens. The field immediately to the left of the lens can be expressed in terms of the field on the object plane $z = z_0$ using the one-dimensional form of Fresnel's formula which, for $z < z_0 + d_{x1}$, gives

$$E_1(x, z) = \sqrt{\frac{1}{+j\lambda(z - z_0)}} \int_{-\infty}^{\infty} E_1(x_0, z_0) \exp\left[-jk\frac{(x - x_0)^2}{2(z - z_0)}\right] dx_0. \tag{27}$$

By multiplying the field immediately to the left of the lens by the factor

$$\exp\left(-jk\frac{x^2}{2f_1}\right),$$

we obtain the field immediately to the right, which can then be used (with the help of Fresnel's formula) to determine the field over the image plane $z = z_1$. The resulting expression gives the result

$$E_1(x_1, z_1) = \frac{1}{+j}\sqrt{\frac{d_{x1}}{d_{x2}}}\,E_1\left(-\frac{d_{x1}}{d_{x2}}x_1, z_0\right)\exp\left(jk\frac{x_1^2}{2f_1}\frac{d_{x1}}{d_{x2}}\right), \quad (28)$$

as we may verify by using the procedure of Ref. 6.

Next, consider the two-dimensional case of Fig. 13b where f_1, f_2 now satisfy eq. (26) and

$$\frac{1}{d_{y1}} + \frac{1}{d_{y2}} = \frac{1}{f_2}, \quad (29)$$

and assume that over the plane $z = z_0$, E_y is of the type

$$E_y(x, y, z) = \psi_1(x)\psi_2(y)e^{jkz_0}, \qquad \text{for} \quad z = z_0. \quad (30)$$

Then, using the two-dimensional form of Fresnel's formula we find that for any $z > z_0$ the distributions of E_y in the x- and y-directions can be treated separately, and each distribution can be determined using the one-dimensional form of Fresnel's formula. More precisely, E_y can be written in the form

$$E_y(x, y, z) = E_1(x, z)E_2(y, z)e^{jkz}, \quad (31)$$

and the relation between $E_1(x, z)$ and $E_1(x, 0)$ [or between $E_2(y, z)$ and $E_2(y, 0)$] can be found considering the one-dimensional problem of Fig. 13a (replacing, in the case of E_2, d_{x1}, d_{x2}, f_1 in Fig. 13a with d_{y1}, d_{y2}, f_2). Thus, using eq. (28), we find

$$E_y(x_1, y_1, z_1)e^{-jkz_1} = -\sqrt{\frac{d_{x1}d_{y1}}{d_{x2}d_{y2}}}\,E_y\left(-\frac{d_{x1}}{d_{x2}}x_1, -\frac{d_{y1}}{d_{y2}}y_1, z_0\right)$$
$$\cdot\exp\left(jk\frac{x_1^2}{2f_1}\frac{d_{x1}}{d_{x2}}\right)\exp\left(jk\frac{y_1^2}{2f_2}\frac{d_{y1}}{d_{y2}}\right). \quad (32)$$

Note that, because of eqs. (26) and (29), the object and image planes ($z = z_0$ and $z = z_1$, respectively) are conjugate planes. All rays emanating from a point (x_0, y_0) in the object plane intersect each other at the conjugate point (x_1, y_1) in the image plane where x_1 and y_1 are

related to x_0 and y_0 by the magnifications

$$M_x = \frac{x_1}{x_0} = -\frac{d_{x2}}{d_{x1}} \quad \text{and} \quad M_y = \frac{y_1}{y_0} = -\frac{d_{y2}}{d_{y1}}.$$

Equation (32), derived for the particular case of eq. (30), is valid also for arbitrary $E_y(x, y, z_0)$, as may be seen by writing $E_y(x, y, z_0)$ in the form

$$E_y(x, y, z_0) = \sum A_{mn}\psi_{1m}(x)\psi_{2n}(y)e^{jkz_0}, \tag{33}$$

and then applying eq. (32) to each term of this expression. Equation (32) can also be derived using eq. (15a) of Ref. 7. If one conjugate plane, $z = z_1$, is in the far field, eq. (32) gives eq. (7).

APPENDIX B

In this appendix the field radiated by the corrugated horn is represented in terms of Laguerre-gaussian modes of propagation.[10] Let the truncated Bessel function

$$\psi = \begin{cases} J_0(u), & |u| \leqq u_{a0} \\ 0, & |u| > u_{a0} \end{cases} \tag{34}$$

be developed into Laguerre-gaussian functions

$$\psi = \sum_{m=0}^{\infty} B_m L_m\left(\frac{u^2}{\bar{u}^2}\right) \exp\left(-\frac{u^2}{2\bar{u}^2}\right), \tag{35}$$

where L_m are Laguerre polynomials,

$$L_m(x) = \frac{e^x}{n!}\frac{d^n}{dx^n}(e^{-x}x^n), \tag{36}$$

and $\bar{u}$ is a parameter whose optimum choice is, for the present purpose, that which maximizes the ratio

$$\eta = \frac{B_0^2}{\sum_0^{\infty} B_k^2}.$$

We can show that η is maximum for

$$\bar{u} = 1.09549, \tag{37}$$

and that

$$\eta_{\max} = 0.9811. \tag{38}$$

We therefore assume this particular value of $\bar{u}$.

We now derive the field E_y for $z > 0$ subject to the boundary condition

$$E_y(x, y, 0) = \psi \exp\left[j \frac{k}{2R} (x^2 + y^2)\right] \tag{39}$$

for $z = 0$. We assume that Fresnel's formula is applicable, which implies that the wave equation $(\partial^2/\partial x^2 + \partial^2/\partial y^2 + \partial^2/\partial z^2 + k^2)E_y = 0$ can be approximated by the parabolic wave equation

$$[k^2 + \tfrac{1}{2}(\partial^2/\partial x^2 + \partial^2/\partial y^2)]E_y = -jk\partial E_y/\partial z.$$

We can verify that the solution of the parabolic wave equation that satisfies the above boundary condition is given by[10]

$$E_y(x, y, z) = e^{jkz} \sum_0^\infty B_m C_m L_m \left(\frac{k(x^2 + y^2)}{A}\right) \exp\left[j \frac{k}{2q} (x^2 + y^2)\right], \tag{40}$$

where C_m, A, and q are functions of z,

$$q = q(z) = q(0) + z \tag{41}$$

$$\frac{1}{A} = \mathrm{IM}\left(\frac{1}{q}\right) \tag{42}$$

$$C_m = \sqrt{\frac{A_0}{A}} \left[\frac{\dfrac{z}{q(0)^*} + 1}{\dfrac{z}{q(0)} + 1}\right]^{m+\frac{1}{2}}, \tag{43}$$

and $A_0 = A$ for $z = 0$. The complex beam parameter $q(0)$ appearing in these formulas is determined by the feed characteristics,

$$\frac{1}{q(0)} = j \frac{1}{(ka)^2} \frac{ku_{a0}^2}{\bar{u}^2} + \frac{1}{R}. \tag{44}$$

We can verify by means of eqs. (35) and (40) to (44) that E_y satisfies condition (39) for $z = 0$.

In the experiment, the focal plane is behind the aperture of the feed. In this case, to derive the far field using eq. (7) we have to consider not the field radiated by the feed in the half space $z > 0$, but its virtual extension into the half space $z < 0$. We can show, however, that eq. (40) is valid also in this case (i.e., for $z = z_0 < 0$).

According to eq. (38), 98.11 percent of the total energy radiated by the feed is caused by the fundamental gaussian mode (18), which is the term $m = 0$ of eq. (35). Therefore, the horn is an efficient gaussian

beam launcher, and a rough estimate of the radiation characteristics of the feed and the antenna can be obtained considering only this $m = 0$ term. In this case using eqs. (7) and (8) we obtain, for the 3-dB beamwidths $2\theta_1$ and $2\theta_2$ of the antenna in the two principal planes,[10,11]

$$2\theta_1 = \sqrt{2 \ln 2}\,\frac{w_0}{f_1} \tag{45}$$

$$2\theta_2 = \sqrt{2 \ln 2}\,\frac{w_0}{f_2}, \tag{46}$$

with w_0 given by eq. (21). The beamwidth $2\theta_f$ of the feed pattern is[10]

$$2\theta_f \cong \frac{\lambda}{\pi w_0}\sqrt{2 \ln 2}. \tag{47}$$

The distance z_0 of the phase center from the feed aperture is[10] given by eq. (20).

The spot size* of the gaussian beam at the horn aperture is[10]

$$w = \sqrt{\frac{\lambda A_0}{\pi}} = \sqrt{2}\left(\frac{\bar{u}a}{u_{a0}}\right) \cong 0.6437\ a. \tag{48}$$

APPENDIX C

Derivation of Eq. (11)†

It can be shown[1,2] that the far field of the feed of Section 2.2 has, because of boundary condition (10), the following property: If the far field is transformed into a plane wave using an optical system of revolution centered around the feed axis, then the resulting plane wave is vertically polarized if the input of the feed is vertically polarized. We now show that this property implies condition (11).

Consider an optical system of revolution centered around the z-axis, and let (ρ, ϕ) be polar coordinates defined by $x = \rho \cos \phi$, $y = \rho \sin \phi$. Consider an input ray entering the optical system with direction parallel to the axis of symmetry and with polarization characterized by unit vector e_0. Let the meridional plane defined by this ray be the plane $\phi = \phi_0$ (see Fig. 14). Because of the symmetry of the system, this ray will be transformed into an output ray leaving the system in the same meridional plane $\phi = \phi_0$. Therefore, if (k_x, k_y, k_z) is the wave vector characterizing the direction of the output ray and θ_1 is the angle between (k_x, k_y, k_z) and the z-axis (see Fig. 14),

* Spot size is defined (Ref. 10) as the radius at which the field amplitude drops to $1/e$ of its value on axis.

† See Chapter VI of Ref. 12 for a justification of the approach used in this derivation.

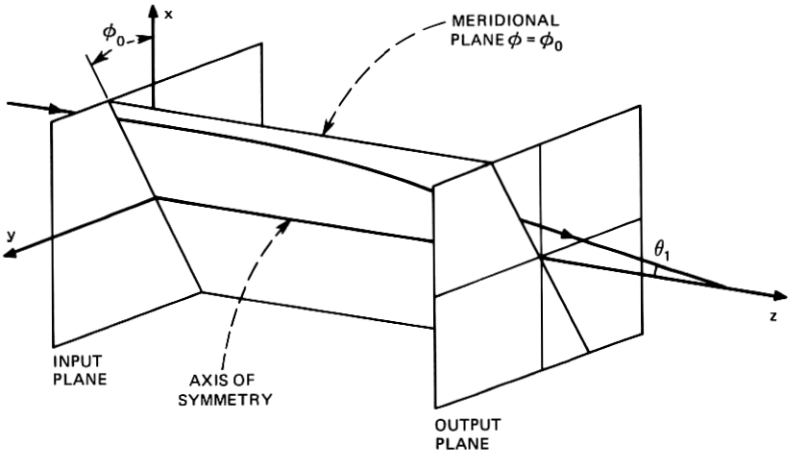

Fig. 14—Transformation by an optical system of revolution of an input ray incident parallel to the axis of symmetry.

then

$$\begin{aligned} k_x &= -k \sin \theta_1 \cos \phi_0 \\ k_y &= -k \sin \theta_1 \sin \phi_0 \\ k_z &= k \cos \theta_1. \end{aligned} \tag{49}$$

Now if e_1 is a unit vector characterizing the polarization of the output ray, there is a simple relation between e_1 and e_0 that can be obtained as follows. The ray in question, as it passes through the system, describes a plane curve since it remains in the plane $\phi = \phi_0$. It immediately follows that if e_0 lies in the plane $\phi = \phi_0$ then e_1 must lie in this plane also, while if e_0 is orthogonal to it, then e_1 is also. In other words,

$$\begin{aligned} e_1 &= i_\phi && \text{if} \quad e_0 = i_\phi \\ e_1 &= \cos \theta_1 i_\rho + \sin \theta_1 i_z && \text{if} \quad e_0 = i_\rho, \end{aligned}$$

where i_ϕ and i_ρ are unit vectors in the ϕ, ρ-directions. From these two relations it follows that, if the input ray is polarized in the y-direction,

$$e_0 = \sin \phi_0 i_\rho + \cos \phi_0 i_\phi,$$

then

$$e_1 = \sin \phi_0 (\cos \theta_1 i_\rho + \sin \theta_1 i_z) + \cos \phi_0 i_\phi. \tag{50}$$

Now the field along the output ray can be written in the form

$$E = e_1 A e^{j\psi},$$

where A is approximately constant and

$$\psi = k_x x + k_y y + k_z z. \tag{51}$$

We now determine the x, y-components of E using eq. (51) and the relations $i_\rho \cdot i_x = \cos \phi_0$, $i_\phi \cdot i_x = -\sin \phi_0$, $i_\rho \cdot i_y = \sin \phi_0$, $i_\phi \cdot i_y = \cos \phi_0$. The result is

$$E_x = \sin \phi_0 \cos \phi_0 (\cos \theta_1 - 1) A e^{j\psi}$$
$$E_y = [1 + \sin^2 \phi_0 (\cos \theta_1 - 1)] A e^{j\psi}.$$

From these relations and eqs. (50) and (52), we can verify with little difficulty that for small θ_1

$$E_x \cong -\sin \phi_0 \cos \phi_0 \frac{\sin^2 \theta_1}{2} A e^{j\psi} \cong \frac{1}{2k^2} \frac{\partial^2 E_y}{\partial x \partial y}. \tag{52}$$

Now we assume that the angle θ_1, which is a function of the distance ρ_0 of the input ray from the z-axis, remains small for all ρ_0. Then, according to eq. (53), a plane wave polarized in the y-direction is transformed by the optical system into a wave satisfying eq. (11).

Equation (53) was derived by ray optics that apply in the far field of the feed. However, if a differential relation such as (52) holds in the far field, it must hold everywhere (e.g., in the aperture plane of the feed horn).

REFERENCES

1. H. C. Minett and B. MacA. Thomas, "A Method of Synthesizing Radiation Patterns with Axial Symmetry," IEEE Trans., *AP-14*, 1966, pp. 645–656.
2. V. H. Rumsey, "Horn Antennas with Uniform Power Patterns Around their Axes," IEEE Trans., *AP-14*, 1966, pp. 656–658.
3. T. S. Chu and R. H. Turrin, "Depolarization Properties of Off-Set Reflector Antennas," IEEE Trans. on Antennas and Propagation, *AP-21*, No. 3 (May 1973), pp. 339–345.
4. R. C. Spencer, F. S. Holt, H. M. Johanson, and J. Sampson, "Double Parabolic Cylinder Pencil-Beam Antenna," IRE Trans. on Antennas and Propagation, January 1955, pp. 4–8.
5. L. C. Tillotson, "Use of Frequencies above 10 GHz for Common Carrier Applications," B.S.T.J., *48*, No. 6 (July-August 1969), pp. 1563–1576.
6. H. Kogelnik, "Imaging of Optical Modes-Resonators with Internal Lenses," B.S.T.J., *44*, No. 3 (March 1965), pp. 455–494.
7. J. A. Arnaud, "Nonorthogonal Optical Waveguides and Resonators," B.S.T.J., *49*, No. 9 (November 1970), pp. 2311–2347.
8. G. A. Deschamps, "Gaussian Beam as a Bundle of Complex Rays," Electron. Lett., *7*, No. 23 (1971), pp. 684–685.
9. P. J. B. Clarricoats and P. K. Saha, "Propagation and Radiation Behaviour of Corrugated Feeds," Proc. IEE, *118*, No. 9 (September 1971), pp. 1167–1176.
10. H. Kogelnik and T. Li, "Laser Beams and Resonators," Appl. Opt., *5*, No. 10 (October 1966), pp. 1550–1567.
11. G. Goubau, "Optical Relations for Coherent Wave Beams," *Electromagnetic Theory and Antennas*, E. C. Jordan, ed., New York: Pergamon Press, 1963.
12. R. K. Luneburg, *Mathematical Theory of Optics*, Berkeley: University of California Press, 1966.